HHS Public Access

Author manuscript

Nat Med. Author manuscript; available in PMC 2012 October 01.

Published in final edited form as:

Nat Med. ; 18(4): 600–604. doi:10.1038/nm.2679.

Activation of neuronal P2X7 receptor-Pannexin-1 mediates death of enteric neurons during colitis

Brian D. Gulbransen[1,2,3], **Mohammad Bashashati**[1,2,3], **Simon A. Hirota**[3,4,5,6], **Xianyong Gui**[7], **Jane A. Roberts**[8], **Justin A. MacDonald**[3,5,6], **Daniel A. Muruve**[3,4], **Derek M. McKay**[2,3], **Paul L. Beck**[3,4], **Gary M. Mawe**[8], **Roger J. Thompson**[1,9], and **Keith A. Sharkey**[1,2,3]

[1]Hotchkiss Brain Institute, University of Calgary, 3330 Hospital Drive NW Calgary, Alberta, T2N 4N1 Canada

[2]Department of Physiology and Pharmacology, University of Calgary, 3330 Hospital Drive NW Calgary, Alberta, T2N 4N1 Canada

[3]Snyder Institute of Infection, Immunity and Inflammation, University of Calgary, 3330 Hospital Drive NW Calgary, Alberta, T2N 4N1 Canada

[4]Department of Medicine, University of Calgary, 3330 Hospital Drive NW Calgary, Alberta, T2N 4N1 Canada

[5]Libin Cardiovascular Institute, University of Calgary, 3330 Hospital Drive NW Calgary, Alberta, T2N 4N1 Canada

[6]Department of Biochemistry and Molecular Biology, University of Calgary, 3330 Hospital Drive NW Calgary, Alberta, T2N 4N1 Canada

[7]Department of Pathology and Laboratory Medicine, University of Calgary, 3330 Hospital Drive NW Calgary, Alberta, T2N 4N1 Canada

[8]Department of Anatomy & Neurobiology, University of Vermont College of Medicine, 89 Beaumont Avenue, Burlington, VT, 05405 USA

[9]Department of Cell Biology and Anatomy, University of Calgary, 3330 Hospital Drive NW Calgary, Alberta, T2N 4N1 Canada

Abstract

Inflammatory bowel diseases (IBD) are chronic relapsing and remitting conditions associated with long-term gut dysfunction resulting from alterations to the enteric nervous system and a loss of enteric neurons[1,2]. The mechanisms underlying inflammation-induced enteric neuron death are

To whom correspondence should be addressed: bgulbran@ucalgary.ca (BDG); ksharkey@ucalgary.ca (KAS).

Author contributions: Overall project design and hypotheses were developed by B. Gulbransen under the supervision of R. Thompson and K. Sharkey. B. Gulbransen coordinated the project, conducted all experiments unless otherwise noted, analyzed the data, prepared figures and wrote the manuscript. M. Bashashati carried out the colon contractility experiments. P. Beck, X. Gui, S. Hirota, J. Roberts, J. MacDonald, D. Muruve, D. McKay and G. Mawe contributed to experimental design, prepared and provided animals, tissues and reagents. All authors participated in revising the manuscript and agreed to the final version. R. Thompson and K. Sharkey supervised the overall project.

unknown. Here we report using *in vivo* models of experimental colitis that inflammation causes enteric neuron death by activating a neuronal signaling complex comprised of P2X7 receptors (P2X7Rs), pannexin–1 (Panx1) channels, Asc and caspases. Inhibiting P2X7Rs, Panx1, Asc or caspase activity prevents inflammation-induced neuron cell death. Preservation of enteric neurons by inhibiting Panx1 *in vivo* prevented the onset of inflammation-induced colonic motor dysfunction. Panx1 expression is reduced in Crohn's disease but not ulcerative colitis. We conclude that activation of neuronal Panx1 underlies neuron death and subsequent development of the abnormal gut motility in IBD. Targeting Panx1 represents a novel neuroprotective strategy to ameliorate the progression of IBD–associated dysmotility.

Six keywords

myenteric plexus; purinergic; enteric glia; inflammation; colonic motility; enteric nervous system

Numerous gastrointestinal disorders are associated with abnormal motility, leading to severe and debilitating symptoms. Despite the view that enteric neurodegeneration or functional impairment of neurons underlies dysmotility in these disorders[1,2], the causal mechanisms culminating in neuron death are unresolved. Thus, no neuroprotective therapeutic strategies exist to preserve gastrointestinal function and current treatment options are limited to controlling inflammation, frequently leaving patients with chronic gut dysfunction.

Altered purinergic signaling is a key–contributing factor to the pathophysiology of IBD. Increased release[3,4] and reduced hydrolysis[3,5] elevate extracellular purines during inflammation and purine receptor genes and proteins are dysregulated in affected humans[6,7] and animal models[8]. Experimentally increasing extracellular purines exacerbates colitis[9] and impaired purine hydrolysis is associated with increased susceptibility to colitis in humans[5]. Constitutively elevated extracellular ATP during inflammation contributes to cytotoxicity by chronically activating P2X7Rs[10–12], triggering neuronal death[10,13–15]. Because enteric neurons are rapidly lost when inflammation is initiated and this occurs prior to immune function[16], we tested the hypothesis that direct activation of signaling cascades by enteric neuronal P2X7Rs mediates their death during inflammation. We find robust P2X7R-immunoreactivity (ir) localized to neurons throughout the myenteric plexus of the mouse colon (Fig. 1a) and that inflammation induces a rapid loss of enteric neurons in multiple models of colitis (Fig. 1b). We next assessed the neuroprotective effects of inhibiting P2X7Rs during inflammation with the antagonist, oxidized–ATP (o–ATP; 7.5 mg kg^{-1}; i.p.). Without o–ATP, mouse myenteric neuronal density decreased by 32±8% during colitis (Fig. 1c-d). Pre–treatment with o–ATP protected against inflammation–induced neuron loss (Fig. 1c-d) without affecting macroscopic damage scores or weight loss patterns (Fig. 1e-f). Thus, neuronal P2X7Rs are necessary for neurodegeneration during colitis but not the inflammatory response *per se*.

Is P2X7R activation sufficient to drive neuron death? When we challenged whole–mount preparations of mouse colonic myenteric plexus with the selective P2X7R agonist BzATP (300 μM, 2 h) and assessed neuronal survival; neural packing density was reduced by 34±2% (Fig. 1g), closely resembling the *in vivo* situation. No immune cells were observed

in, or adjacent to, myenteric ganglia in histological evaluation of whole–mounts (Supplementary Fig. 1), ruling out the possibility that BzATP-mediated neuron death is secondary to immune cell P2X7R activation.

Cell death in P2X7R–expressing oocytes depends on co–expression with Panx1[17]. Inhibiting Panx1 with the selective small peptide inhibitor, ^{10} panx (100 μM)[18,19], completely protected against BzATP–induced neuronal death while the scrambled version of the ^{10} panx peptide (scPeptide) was without effect (Fig. 1g). In cultured macrophages, P2X7R stimulation contributes to cell death by activating multiple caspases[20] and subsequent IL–1β release[21]. P2X7R–mediated enteric neuron death required caspases, but not IL–1β, because neuronal death was prevented by the pan–caspase inhibitor zVAD(OMe)–fmk (zVAD; 80 μM) (Fig. 1g). In contrast, treatment with the IL–1 receptor antagonist (IL-1-ra, Anakinra; 1500 ng/mL) was not neuroprotective (Fig. 1g).

The immunohistochemical distribution of Panx1 in the mouse colon showed localization on the cell bodies and processes of enteric neurons (Fig. 2a) but not glia, as evident by the intimate association of GFAP-ir glia with Panx1-ir neurons (Fig. 2a). Importantly, Panx1–expressing myenteric neurons also co–express P2X7Rs (Supplementary Fig. 2), and 51% were identified as nNOS–ir and 40% as calretinin–ir (Supplementary Fig. 2).

Inhibiting Panx1 during DNBS–colitis *in vivo* with probenecid (PB, 177.5 mg kg^{-1}, i.p.)[22,23] preserved normal neural packing density without modifying the underlying tissue inflammation (Fig. 2b, d–e). Daily probenecid injections also protected against the 24±4% decrease in myenteric neuron packing density in the DSS–colitis model (Fig. 2b), but not the oxazolone model of ulcerative colitis.

In vivo Panx1 opening may contribute to neuron death by activating a large protein complex termed the inflammasome[23]. We tested if inflammasome activation is required for neuron death *in vivo* using mice deficient in either the adaptor protein Asc (apoptosis–associated speck–like protein containing a CARD; *Pycard*$^{-/-}$) or Nlrp3 (nucleotide–binding domain and leucine–rich repeat containing gene family pyrin domain containing 3; *Nlrp3*$^{-/-}$). Weight loss and macroscopic damage in *Pycard*$^{-/-}$and *Nlrp3*$^{-/-}$mice were similar to wild–type mice treated with DNBS (Fig. 2d–e). However, *Pycard*$^{-/-}$DNBS–treated mice failed to lose enteric neurons whereas density was significantly (P<0.0001) reduced 23±3% in *Nlrp3*$^{-/-}$DNBS–treated mice (Fig. 2b). Therefore, P2X7R–Panx1–mediated enteric neural death depends on Asc activation of caspases independent of Nlrp3. Indeed, Asc was ubiquitously expressed by enteric neurons (Fig. 2c), but Nlrp3–ir was not evident (data not shown).

Panx1 acts as a conduit for ATP release from apoptotic cells to recruit phagocytes[24]. Therefore, we tested if Panx1 opening, activated by P2X7R, stimulates ATP release from enteric neurons using the highly ATP–responsive enteric glia[25] surrounding enteric neurons as endogenous “sniffer cells”.

Bath application of the P2X7R agonist BzATP (100 μM) stimulated Ca^{2+} responses in neurons, followed closely (by 6.75±1 s) by Ca^{2+} responses in surrounding enteric glia (Supplementary Fig. 3a–b and Supplementary Video 1). Indicative of P2X7Rs, BzATP

responses in neurons and glia were potentiated by lowering extracellular Ca^{2+} and Mg^{2+}, unaffected by TTX (1 μM) and blocked by the P2X7R antagonists o-ATP (100 μM) and A438079 (30 μM) (Supplementary Figs. 3–4). Extrinsic nerve fibers do not express P2X7Rs and neuronal and glial responses remained unchanged after specifically ablating sympathetic innervation or in cultured preparations devoid of all extrinsic innervation (Supplementary Fig. 5).

In mice, enteric glia respond to ATP through a phospholipase C (PLC) signaling cascade initiated by P2Y1Rs[25,26]. If glial responses to BzATP are due to ATP release from neurons, then inhibiting either PLC or P2Y1Rs should preferentially block glial responses to BzATP. In support, the PLC inhibitor U73122 (10 μM) and the P2Y1R antagonist MRS2179 (10 μM) completely blocked glial responses to BzATP with no significant inhibitory effect on neurons (Supplementary Fig. 3e, i). Similarly, blocking the extracellular conversion of neuronally–released ATP to ADP (the endogenous ligand for glial P2Y1Rs) by inhibiting ectonucleotidases [POM1 (50 μM)] abolished glial responses without affecting neuronal responses (Supplementary Fig. 3f, i). In summary, enteric neurons release ATP following P2X7R stimulation.

We next asked if P2X7R-stimulated ATP release from enteric neurons depends on Panx1. Inhibiting Panx1 with 2 mM PB[22,23] reduced glial responses to BzATP by 50±12% (Supplementary Fig. 3g, i). The more specific peptide inhibitor ^{10} panx (100 μM) significantly ($P<0.0001$) inhibited glial responses to BzATP by 46±11% without affecting neural responses (Supplementary Fig. 3h–i). From these results we conclude that P2X7R stimulation of enteric neurons elicits a direct release of ATP onto glia through Panx1.

Inflammation–induced impairments in inhibitory enteric neuromuscular transmission in the colon may contribute to the long–term alterations in gastrointestinal motility that persist following inflammation resolution[27–33]. In support, we found a 35% reduction in nNOS–ir neurons during experimental colitis in mice and a substantive decrease in nNOS–ir myenteric neurons in tissue from subjects with Crohn's disease, but no change in subjects with ulcerative colitis (Fig. 3a–c). Decreased nitrergic innervation in experimental colitis was associated with a persistent decrease in electrical field stimulation (EFS)–elicited colon relaxations and enhanced EFS–elicited contractions (Fig. 3d–e). Sensitivity to L–NAME but not suramin confirmed relaxations were nitrergic and not purinergic (Supplementary Fig. 6). Muscle responsiveness was not altered because responses to the muscarinic agonist, bethanechol (10 μM) and the NO donor, sodium nitroprusside (SNP, 100 μM) were unchanged in inflamed colons (Fig. 3f–g). Panx1–mediated neuroprotection during colitis preserved both normal colonic relaxations and contractions following colitis (Fig. 3d–e), suggesting that inhibiting Panx1–mediated neuronal death during colitis could be therapeutically useful to preserve functional innervation and control of colonic muscle.

IBDs are clinically relapsing–remitting conditions and therapeutic intervention occurs after an initial bout of inflammation. To test the potential clinical relevance of Panx1–inhibition as a therapeutic strategy we developed a mouse model of recurrent colitis (Supplementary Fig. 7). After a second bout of colitis, neuron packing density decreased by 28±3% in mice treated with saline during the remission period (Fig. 4a). PB intervention during remission

significantly ($P<0.05$) improved neuron survival and protected against further neuron loss during recurrent inflammatory bouts (Fig. 4a).

To further the clinical significance of our findings, we assessed P2X7R and Panx1 expression in full thickness sections from human colon. Both myenteric and submucosal neurons in the human colon robustly express P2X7Rs (Fig. 4b) and Panx1 (Fig. 4c–e). Importantly, changes in Panx1–ir in tissue from subjects with IBD mirror that of nNOS, with a marked loss of Panx1–ir in the myenteric plexus from subjects with Crohn's disease and no change in ulcerative colitis (Fig. 4f).

Collectively, our work identifies a critical mechanism of neuron death in intestinal inflammation that appears relevant in Crohn's disease. Our data support a model whereby elevated levels of extracelluar ATP chronically activates neuronal P2X7Rs, Panx1 and caspases, leading to preferential loss of nitrergic neurons (**Fig. 6g**). We identify Panx1 as a key molecular substrate underlying enteric neural damage, leading to organ dysfunction following colitis, and our findings demonstrate that Panx1 inhibition protects neurons and preserves functional control of the colonic musculature. Thus, Panx1 is a novel therapeutic target for the treatment of dysfunction in IBD and possibly other gastrointestinal disorders with an inflammatory component.

METHODS

Animals

Our protocols adhered to the guidelines of the Canadian Council on Animal Care and were approved by the University of Calgary Animal Care and Use Committee. We used male C57Bl/6 mice (6–12 weeks old; Charles River) in all studies except when transgenic strains were needed. Vishva Dixit (Genetech) and Jurg Tschopp (University of Lausanne) provided male *Pycard*$^{-/-}$and *Nlrp3*$^{-/-}$mice (6–9 weeks old, C57Bl/6 background), respectively. *Il10*$^{-/-}$mice and wild-type littermates were generated as described previously[34].

Human tissue

We obtained full-thickness specimens of normal and diseased human colon after informed consent from a minimum of 3 male subjects with active Crohn's disease, 3 with ulcerative colitis, and 3 undergoing resection for colon cancer. Marginal safe tissue bordering tumorous bowel served as controls. We performed antigen retrieval with sodium citrate (pH 6.0, 80°C, 30 min) on the Holland's fixatived, paraffin–embedded, sections before proceeding with immunohistochemistry.

Induction of colitis

We induced colitis with dinitrobenzene sulphonic acid (DNBS), ozazolone, and dextran sodium sulfate (DSS) as described by Wirtz et al.[35]. We anesthetized mice with isoflurane, inserted a gavage needle 3 cm into the colon and injected 0.1 mL of a solution containing either 5 mg DNBS or oxazolone dissolved in 50% ethanol, or saline alone for controls. We monitored animals closely and recorded weight loss daily for 48 h before sacrificing and scoring macroscopic damage[36]. We induced DSS colitis by adding 3% DSS to drinking

water for 8 d. *Il-10*$^{-/-}$mice spontaneously developed colitis as described previously[34]. We preserved colonic tissue in Zamboni's fixative.

Whole–mount immunohistochemistry

We prepared whole-mount preparations of the colonic myenteric plexus by removing the mucosa, submucosa and circular muscle by microdissection. We processed the resulting longitudinal muscle myenteric plexus (LMMP) preparations for immunohistochemistry as described by Gulbransen and Sharkey[25] with the antibodies listed in Supplementary Table 1. We confirmed antibody specificity by pre-absorption with control peptides or in respective knockout animals.

Ca^{2+} imaging

We prepared tissues as described by Gulbransen *et al.*[37] and acquired images every 1–2 s through the 40X water immersion objective (LUMPlanFl/IR, 0.8 n.a.) of an upright Olympus BX61WI motorized fixed stage microscope (Olympus) using Imaging Workbench 6 software (INDEC BioSystems) and a CCD Hamamatsu ORCA-ER digital camera (Hamamatsu Photonics K.K.). We continually perfused LMMPs at 2–3 mL min^{-1} with buffer (near 33°C) using a gravity flow perfusion system (Automate Scientific Inc.). We dissolved agonists and antagonists in buffer and bath applied agonists for 30 s and antagonists for 15 min. For details on Ca^{2+} imaging analysis, see Supplementary Methods.

In situ P2X7R–stimulated neuron death

We prepared LMMP whole-mounts as for Ca^{2+} imaging, pinned them flat in Sylgard-coated 35 mm dishes, and maintained them in a humid oxygenated chamber at 34°C. We obtained a total of 6 LMMPs from each animal and, of these, incubated 2 in buffer alone, 2 with 300 μM BzATP, and 2 with 300 μM BzATP plus inhibitor for 2 h. We then rinsed tissues with buffer and maintained them in either buffer alone or buffer with inhibitor for an additional 2 h before being fixed with Zamboni's fixative overnight.

Contractility studies

We performed colon contractility studies as described by Nasser *et al.*[38]. For further details, see Supplementary Methods.

Solutions

Modified Krebs buffer (buffer) contained (in mmol L^{-1}): 121 NaCl, 5.9 KCl, 2.5 $CaCl_2$, 1.2 $MgCl_2$, 1.2 NaH_2PO_4, 10 HEPES, 21.2 $NaHCO_3$, 1 pyruvic acid, 8 glucose (Sigma)(pH adjusted to 7.4 with NaOH) with 3 μmol/L nicardipine (Sigma) and 1 μmol L^{-1} scopolamine (Sigma) to inhibit muscle contractions. We prepared low Ca^{2+}/Mg^{2+} buffer as above but lowered $CaCl_2$ to 0.5 and omitted $MgCl_2$. We purchased 2'(3')-O-(4-Benzoyl)adenosine 5'-triphosphate triethylammonium salt (BzATP) and adenosine 5'-triphosphate periodate oxidized sodium salt (o-ATP) from Sigma, A438079, MRS2179, and tetrodotoxin (TTX) from Tocris Bioscience, U73122 from Calbiochem (EMD Chemicals, Inc), probenecid from Invitrogen, and ^{10} panx from AnaSpec.

Data analysis

We acquired images of ganglia with HuC/D–ir or nNOS–ir neurons for counts through the 20X (Plan-Neofluar, 0.5 n.a.) objective of an upright epifluorescence microscope (Zeiss Axioplan, Carl Zeiss) equipped with a Retiga 2000R CCD camera (QImaging) controlled by QCapture Pro 6.0 software (QImaging). We measured ganglionic area and recorded the number of neurons within that area using ImageJ (NIH). We determined neuronal packing density per animal by averaging counts from a minimum of 10 ganglia per animal except for *in situ* experiments were we averaged counts from a minimum of 20 ganglia from 2 LMMPS from each treatment group per animal. We obtained confocal images through the 60X objective (PlanApo N, 1.42 n.a., oil) of an Olympus BX50 Fluoview laser scanning confocal microscope (Olympus).

Statistical analyses

We present all results as mean ± s.e.m. with statistical differences determined by one-way ANOVA (with Tukey's or Newman-Keuls post-test). A P value of <0.05 was considered significant.

Supplementary Material

Refer to Web version on PubMed Central for supplementary material.

Acknowledgments

This work was supported by grants from the Canadian Institutes of Health Research (CIHR, to K. Sharkey, R. Thompsion and D. McKay), Crohn's & Colitis Foundation of Canada [CCFC to D. McKay] and US National Institutes of Health (NIH) grant DK62267 (G. Mawe). B. Gulbransen holds fellowships from the Canadian Association of Gastroenterology (CAG)/CIHR/Fellowship Award and Alberta Innovates-Health Solutions (AI-HS)/CCFC. K. Sharkey is an AI-HS Medical Scientist and holds the CCFC Chair in IBD Research at the University of Calgary. R. Thompson is an AI-HS Scholar. P. Beck is supported by AI-HS, CIHR and CCFC. J. MacDonald is an AI-HS Senior Scholar and Canada Research Chair. D. McKay is an AI-HS Scientist and holds a Canada Research Chair (Tier 1). S. Hirota holds fellowships from CIHR and AI-HS. We thank C. MacNaughton, W. Ho and A. Wang for technical support, D.M. McCafferty (University of Calgary) for providing *Il-10*$^{-/-}$mice, N. Hyman (University of Vermont) and O. Bathe (University of Calgary) for providing tissue samples and J. Bains for reviewing and commenting on the manuscript.

References

1. Mawe GM, Strong DS, Sharkey KA. Plasticity of enteric nerve functions in the inflamed and postinflamed gut. Neurogastroenterol Motil. 2009; 21:481–491. [PubMed: 19368664]
2. De Giorgio R, et al. Inflammatory neuropathies of the enteric nervous system. Gastroenterology. 2004; 126:1872–1883. [PubMed: 15188182]
3. Wynn G, Ma B, Ruan HZ, Burnstock G. Purinergic component of mechanosensory transduction is increased in a rat model of colitis. Am J Physiol Gastrointest Liver Physiol. 2004; 287:G647–657. [PubMed: 15331354]
4. Lomax AE, Mawe GM, Sharkey KA. Synaptic facilitation and enhanced neuronal excitability in the submucosal plexus during experimental colitis in guinea-pig. J Physiol. 2005; 564:863–875. [PubMed: 15774518]
5. Friedman DJ, et al. From the Cover: CD39 deletion exacerbates experimental murine colitis and human polymorphisms increase susceptibility to inflammatory bowel disease. Proc Natl Acad Sci U S A. 2009; 106:16788–16793. [PubMed: 19805374]

6. Rybaczyk L, et al. New bioinformatics approach to analyze gene expressions and signaling pathways reveals unique purine gene dysregulation profiles that distinguish between CD and UC. Inflamm Bowel Dis. 2009; 15:971–984. [PubMed: 19253308]
7. Yiangou Y, et al. ATP-gated ion channel P2X(3) is increased in human inflammatory bowel disease. Neurogastroenterol Motil. 2001; 13:365–369. [PubMed: 11576396]
8. Guzman J, et al. ADOA3R as a therapeutic target in experimental colitis: proof by validated high-density oligonucleotide microarray analysis. Inflamm Bowel Dis. 2006; 12:766–789. [PubMed: 16917233]
9. Atarashi K, et al. ATP drives lamina propria T(H)17 cell differentiation. Nature. 2008; 455:808–812. [PubMed: 18716618]
10. Wang X, et al. P2X7 receptor inhibition improves recovery after spinal cord injury. Nat Med. 2004; 10:821–827. [PubMed: 15258577]
11. Lazarowski ER, Boucher RC, Harden TK. Constitutive release of ATP and evidence for major contribution of ecto-nucleotide pyrophosphatase and nucleoside diphosphokinase to extracellular nucleotide concentrations. J Biol Chem. 2000; 275:31061–31068. [PubMed: 10913128]
12. Sperlagh B, Vizi ES, Wirkner K, Illes P. P2X7 receptors in the nervous system. Prog Neurobiol. 2006; 78:327–346. [PubMed: 16697102]
13. Cavaliere F, Amadio S, Sancesario G, Bernardi G, Volonte C. Synaptic P2X7 and oxygen/glucose deprivation in organotypic hippocampal cultures. J Cereb Blood Flow Metab. 2004; 24:392–398. [PubMed: 15087708]
14. Hu H, et al. Stimulation of the P2X7 receptor kills rat retinal ganglion cells in vivo. Exp Eye Res. 2010; 91:425–432. [PubMed: 20599962]
15. Zhang X, Zhang M, Laties AM, Mitchell CH. Stimulation of P2X7 receptors elevates Ca2+ and kills retinal ganglion cells. Invest Ophthalmol Vis Sci. 2005; 46:2183–2191. [PubMed: 15914640]
16. Linden DR, et al. Indiscriminate loss of myenteric neurones in the TNBS-inflamed guinea-pig distal colon. Neurogastroenterol Motil. 2005; 17:751–760. [PubMed: 16185315]
17. Locovei S, Scemes E, Qiu F, Spray DC, Dahl G. Pannexin1 is part of the pore forming unit of the P2X(7) receptor death complex. FEBS Lett. 2007; 581:483–488. [PubMed: 17240370]
18. Seminario-Vidal L, et al. Rho signaling regulates pannexin 1-mediated ATP release from airway epithelia. J Biol Chem. 2011; 286:26277–26286. [PubMed: 21606493]
19. Thompson RJ, et al. Activation of pannexin-1 hemichannels augments aberrant bursting in the hippocampus. Science. 2008; 322:1555–1559. [PubMed: 19056988]
20. Ferrari D, et al. P2Z purinoreceptor ligation induces activation of caspases with distinct roles in apoptotic and necrotic alterations of cell death. FEBS Lett. 1999; 447:71–75. [PubMed: 10218585]
21. Ferrari D, et al. Extracellular ATP triggers IL-1 beta release by activating the purinergic P2Z receptor of human macrophages. J Immunol. 1997; 159:1451–1458. [PubMed: 9233643]
22. Silverman W, Locovei S, Dahl G. Probenecid, a gout remedy, inhibits pannexin 1 channels. Am J Physiol Cell Physiol. 2008; 295:C761–767. [PubMed: 18596212]
23. Silverman WR, et al. The pannexin 1 channel activates the inflammasome in neurons and astrocytes. J Biol Chem. 2009; 284:18143–18151. [PubMed: 19416975]
24. Chekeni FB, et al. Pannexin 1 channels mediate 'find-me' signal release and membrane permeability during apoptosis. Nature. 2010; 467:863–867. [PubMed: 20944749]
25. Gulbransen BD, Sharkey KA. Purinergic neuron-to-glia signaling in the enteric nervous system. Gastroenterology. 2009; 136:1349–1358. [PubMed: 19250649]
26. Gomes P, et al. ATP-dependent paracrine communication between enteric neurons and glia in a primary cell culture derived from embryonic mice. Neurogastroent Motil. 2009; 21:870–e62.
27. Collins SM. The immunomodulation of enteric neuromuscular function: implications for motility and inflammatory disorders. Gastroenterology. 1996; 111:1683–1699. [PubMed: 8942751]
28. Vasina V, et al. Enteric neuroplasticity evoked by inflammation. Auton Neurosci. 2006; 126–127:264–272.
29. Krauter EM, et al. Changes in colonic motility and the electrophysiological properties of myenteric neurons persist following recovery from trinitrobenzene sulfonic acid colitis in the guinea pig. Neurogastroenterol Motil. 2007; 19:990–1000. [PubMed: 17973636]

30. Bossone C, Hosseini JM, Pineiro-Carrero V, Shea-Donohue T. Alterations in spontaneous contractions in vitro after repeated inflammation of rat distal colon. Am J Physiol Gastrointest Liver Physiol. 2001; 280:G949–957. [PubMed: 11292604]
31. Mizuta Y, Isomoto H, Takahashi T. Impaired nitrergic innervation in rat colitis induced by dextran sulfate sodium. Gastroenterology. 2000; 118:714–723. [PubMed: 10734023]
32. Depoortere I, Thijs T, Peeters TL. Generalized loss of inhibitory innervation reverses serotonergic inhibition into excitation in a rabbit model of TNBS-colitis. Br J Pharmacol. 2002; 135:2011–2019. [PubMed: 11959805]
33. Strong DS, et al. Purinergic neuromuscular transmission is selectively attenuated in ulcerated regions of inflamed guinea pig distal colon. J Physiol. 2010; 588:847–859. [PubMed: 20064853]
34. McCafferty DM, et al. Spontaneously developing chronic colitis in IL-10/iNOS double-deficient mice. Am J Physiol Gastrointest Liver Physiol. 2000; 279:G90–99. [PubMed: 10898750]
35. Wirtz S, Neufert C, Weigmann B, Neurath MF. Chemically induced mouse models of intestinal inflammation. Nat Protoc. 2007; 2:541–546. [PubMed: 17406617]
36. Storr MA, et al. Activation of the cannabinoid 2 receptor (CB2) protects against experimental colitis. Inflamm Bowel Dis. 2009; 15:1678–1685. [PubMed: 19408320]
37. Gulbransen BD, Bains JS, Sharkey KA. Enteric glia are targets of the sympathetic innervation of the myenteric plexus in the guinea pig distal colon. J Neurosci. 2010; 30:6801–6809. [PubMed: 20463242]
38. Nasser Y, et al. Role of enteric glia in intestinal physiology: effects of the gliotoxin fluorocitrate on motor and secretory function. Am J Physiol Gastrointest Liver Physiol. 2006; 291:G912–927. [PubMed: 16798727]

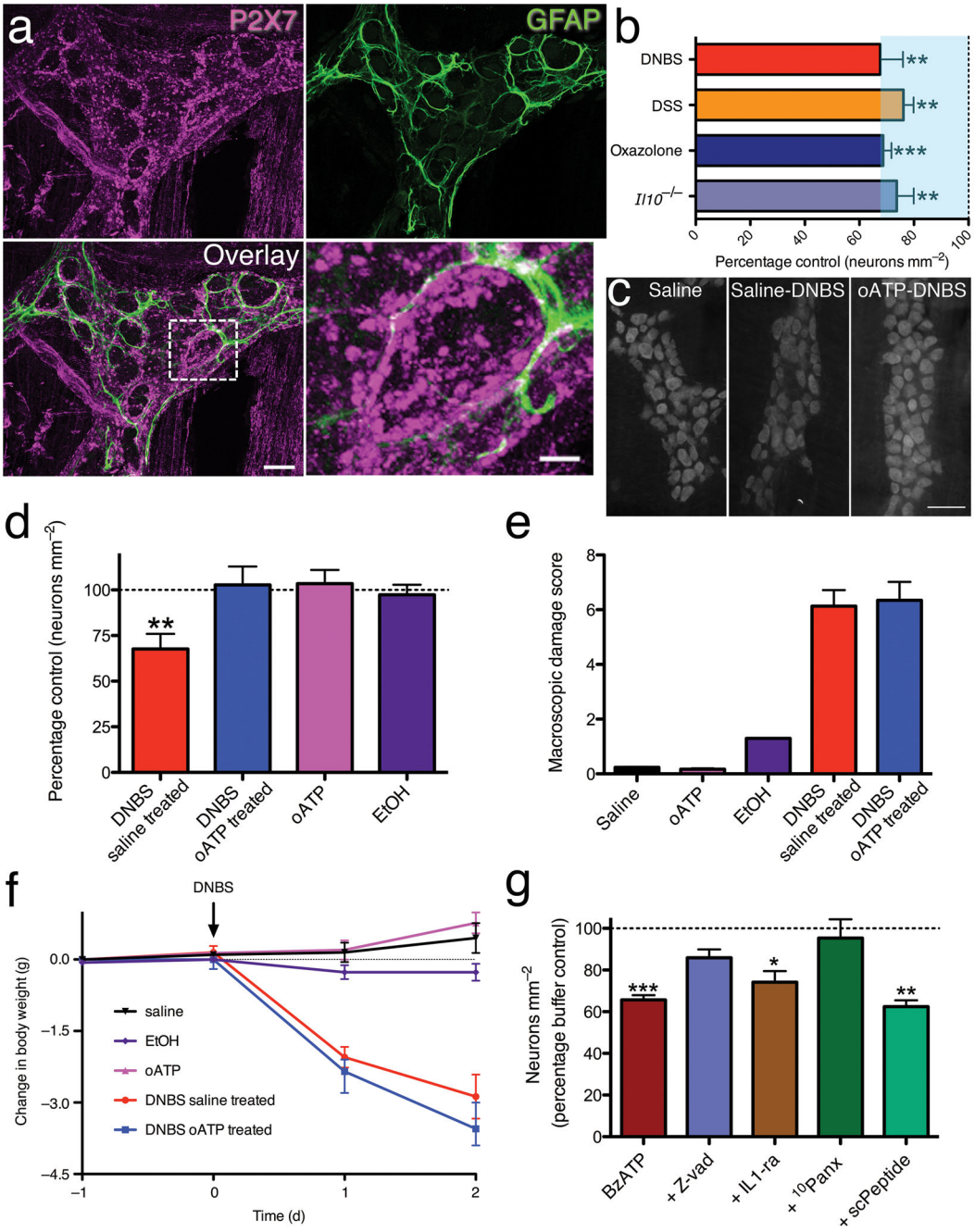

Figure 1.

P2X7R activation is necessary and sufficient for enteric neuron death. (**a**) GFAP (green) and P2X7 (magenta) immunoreactivity in the mouse colon myenteric plexus. (scale bar = 20 μm). Bottom right panel shows an enlarged view of a GFAP–ir glial cell embracing a P2X7–ir enteric neuron (boxed area in overlay). Scale bar = 5 μm. (**b**) Mean packing density of myenteric neurons is significantly reduced in DNBS (2,4-dinitrobenzene sulfonic acid; $n = 4$ animals), DSS (dextran sodium sulfate; $n = 8$), oxazolone ($n = 6$ animals), and interleukin 10 knockout ($I/10^{-/-}$; $n = 4$) models of experimental colitis. ANOVA with $^{**}P < 0.001$ and

***P < 0.0001 versus respective control. (**c**) Representative myenteric ganglia from control (Saline), inflamed (Saline-DNBS), or mice pre-treated with the P2X7R inhibitor oxidized ATP before being inflamed (oATP-DNBS) labeled with the pan-neuronal marker HuC/D (scale bar = 50 μm). (**d**) Mean packing density of HuC/D–ir neurons in the myenteric plexus (**P < 0.001 versus saline, ANOVA, n = 5 animals saline, 4 DNBS saline treated, 3 EtOH, 3 oATP and 4 DNBS oATP treated). Macroscopic damage and weight loss for treatment groups shown in (**e**) and (**f**), respectively. (**g**) Mean packing density of HuC/D–ir neurons after *in situ* activation of P2X7Rs with BzATP alone or with various inhibitors (*P<0.05, **P<0.001, ***P<0.0001 versus buffer, ANOVA, n = 10 animals buffer, 10 BzATP, 3 zVAD, 3 IL-1ra, 3 ^{10}Panx, and 3 scPeptide).

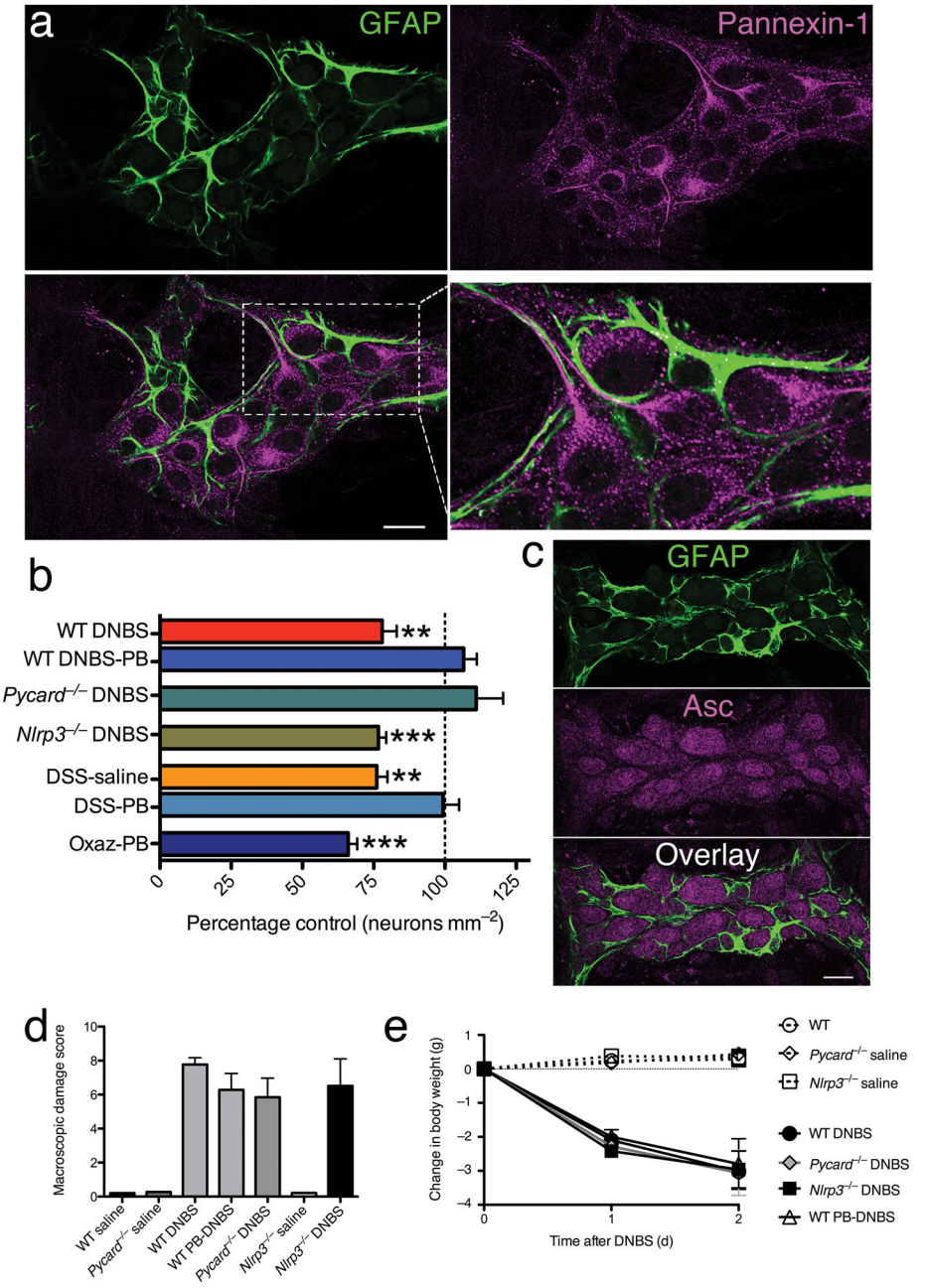

Figure 2.

Inflammation-induced enteric neuron death requires pannexin-1 and Asc but not Nlrp3. (**a**) Pannexin–1 (magenta) and GFAP (green) immunoreactivity in a single optical slice (1 μm) through a myenteric ganglion from the mouse colon myenteric plexus. Enteric glia (GFAP, green) clearly surround pannexin–1–ir (magenta) neural cell bodies and processes. Boxed area in lower left is enlarged in lower right to demonstrate the intimate association between pannexin–1 expressing neurons and enteric glia. Scale bar = 20 μm. (**b**) Effects of inhibiting pannexin–1 or loss of Asc or Nlrp3 on mean packing density of myenteric neurons in DNBS, DSS, and oxazolone models of colitis (Wt DNBS, *n* = 5; Wt DNBS-PB, *n* = 5;

Pycard$^{-/-}$DNBS, $n = 4$; *Nlrp3*$^{-/-}$DNBS, $n = 5$; DSS-saline, $n = 8$; DSS-PB, $n = 5$; Oxaz-PB, $n = 6$). Neural packing density was not significantly different between control animals from the various genetic backgrounds (data not shown). (**c**) Asc (magenta) and GFAP immunoreactivity in the mouse colon myenteric plexus. GFAP–ir glial cells (green) surround Asc–ir neurons (magenta). Macroscopic damage and weight loss for treatment groups in (**b**) shown in (**d**) and (**e**), respectively. Significance determined by ANOVA with ** $P<0.001$ and *** $P<0.0001$ compared to saline–treated, non–inflamed controls.

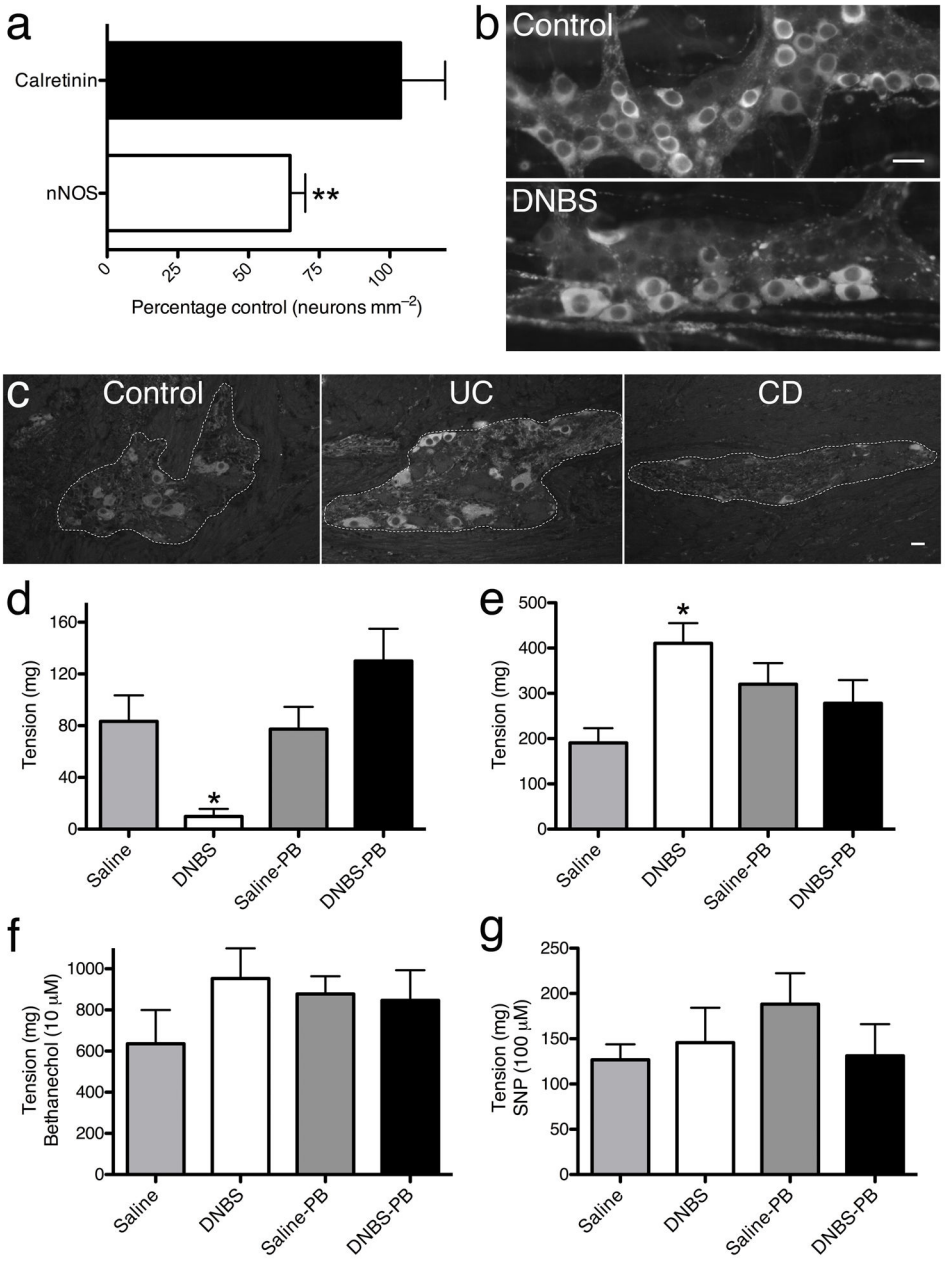

Figure 3.

Inhibiting neuronal pannexin–1 during colitis protects against post–inflammation deficits in inhibitory neuromuscular transmission. (**a**) Mean packing density of nNOS–ir and calretinin–ir neurons in the inflamed mouse colon myenteric plexus (**P< 0.001 compared to saline controls, n = 4, ANOVA. (**b**) Representative photomicrographs showing nNOS-ir neurons in the normal (Control) and inflamed (DNBS) colon myenteric plexus. (**c**) Representative photomicrographs of nNOS labeling within the human myenteric plexus from colonic tissue removed from n = 3 control, 3 ulcerative colitis (UC), and 3 Crohn's disease (CD) subjects. Scale bar = 20 μm. Magnitude of EFS-elicited colon relaxations (**d**) and contractions (**e**) at 21 days post-DNBS in control (Saline, n = 7–8), inflamed (DNBS, n

= 5–7), probenecid treated controls (Saline-PB, *n* = 7–8), or inflamed mice treated with probenecid (DNBS-PB, *n* = 6–8). **P*< 0.05 compared to Saline, ANOVA. (**f**) Muscle responsiveness to the muscarinic agonist bethanechol (10 μM; *n* = 4) and the nitric oxide donor SNP (**g**; 100 μM; *n* = 3) in all groups.

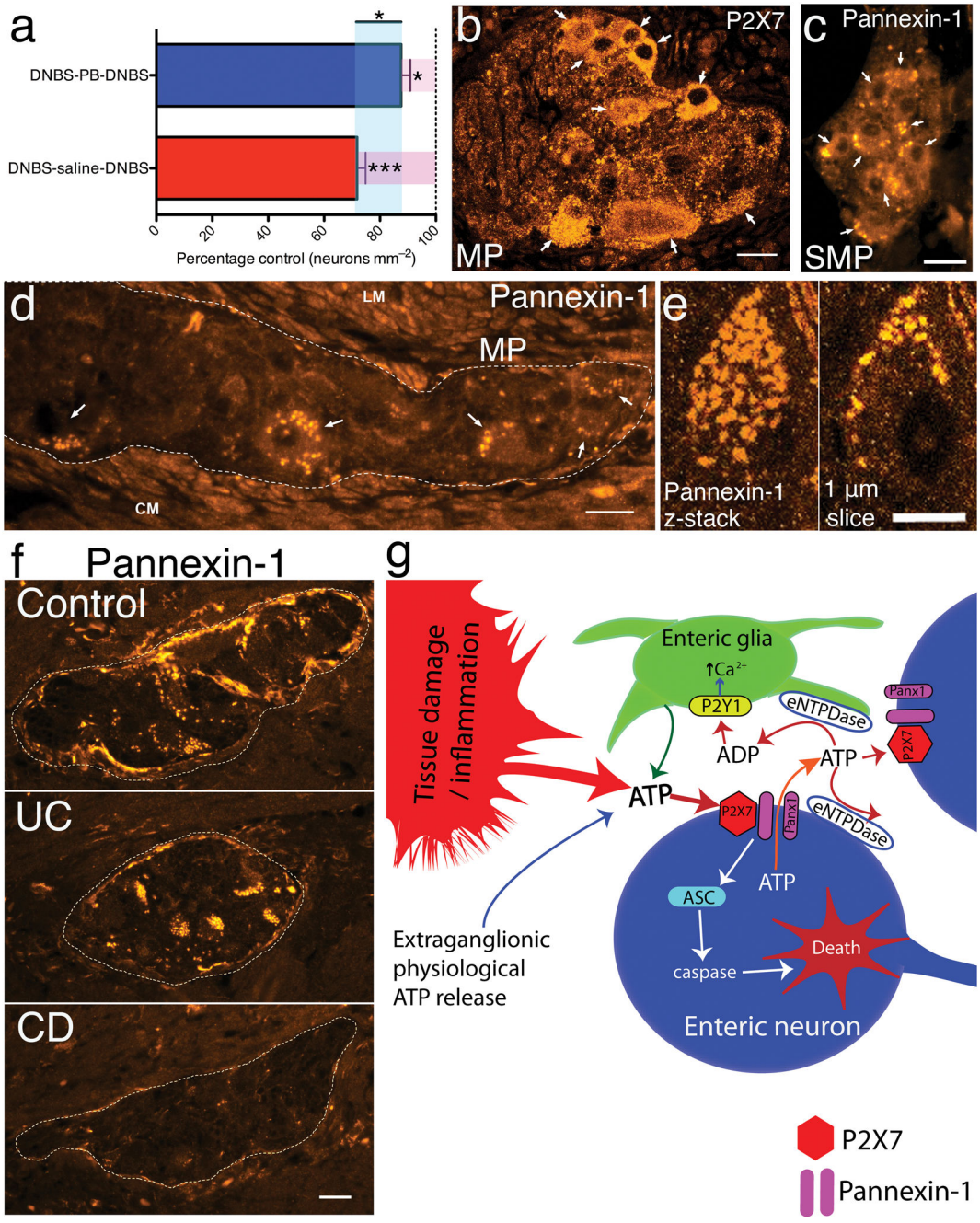

Figure 4.

Pannexin–1 inhibition is neuroprotective in a clinical model of colitis and changes in the P2X7–pannexin–1 pathway expressed by human enteric neurons are involved in the pathophysiology of Crohn's disease. (**a**) Mean myenteric neuron packing density in a mouse model of recurrent colitis comparing treatment with either saline (DNBS–saline–DNBS, n = 6) or probenecid (PB) (DNBS–PB–DNBS, n = 5) in the resolution phase between two bouts of colitis. *P<0.05, ***P<0.0001, ANOVA. (**b**) Numerous neurons express P2X7 (arrows) in the human colon myenteric plexus. (**c–e**) Representative images of pannexin–1–ir in the

human submucosal (**c**) and myenteric (**d**) plexuses of the colon. Dashed line in **d** outlines a myenteric ganglia filled with several pannexin–1–ir neurons (arrows). LM = longitudinal muscle. CM = circular muscle. (**e**) Confocal images of a pannexin–1–ir human myenteric neuron. Pannexin–1–ir appears to covers the neuron in a projection z-stack image (left). A single optical slice (1 μm) through this neuron (right) demonstrates that pannexin–1–ir is confined to the cell surface. Scale bars = 20 μm in **b–d** and **f** and 10 μm in **e**. (**f**) Representative photomicrographs comparing pannexin–1–ir in colonic tissue from human subjects with ulcerative colitis (UC) or Crohn's disease (CD) compared to Controls. (**g**) Model of enteric neuron death during colonic inflammation.